Available online at www.sciencedirect.com
SCIENCE DIRECT®
Catalysis Today 93–95 (2004) 589–594
CATALYSIS TODAY
www.elsevier.com/locate/cattod

Copper doping in titanium oxide catalyst film prepared by dc reactive magnetron sputtering

Wenjie Zhang [a,b,*], Ying Li [a], Shenglong Zhu [a], Fuhui Wang [a]

[a] *State Key Laboratory for Corrosion and Protection, Institute of Metal Research, Chinese Academy of Sciences, Shenyang 110016, China*
[b] *Shenyang Institute of Technology, Shenyang 110016, China*

Available online 1 July 2004

Abstract

Copper-doped titanium oxide films were prepared by dc magnetron sputtering using Ti and Cu mixed target. The XPS spectra showed that titanium was in the Ti^{4+} oxidation state and oxygen was in the form of O^{2-} in TiO_2 and CuO. Apparent high-intensity shake-up satellites of the main Cu 2p peaks indicated the existence of fully oxidized CuO in the Cu-doped TiO_2 films. When the copper concentration was low, the Cu-doped TiO_2 film had the similar anatase phase as pure TiO_2. The samples became amorphous when copper concentration was more than 15.17 at.%. Copper oxides were in the amorphous state in all the films. In the sequence of decreasing copper concentration, the surface morphologies changed from flat to nano-crystalline with nano-sized pores. The absorption edges of the Cu-doped samples shifted to longer wavelength region and the optical transmittances of these films decreased abruptly with increasing copper concentration. The Cu-doped TiO_2 films had different photocatalytic behavior in accordance with the amount of doped copper. The best copper doping concentration was 1.45 at.% in sample I, relating to the most effective photocatalytic activity.

Keywords: TiO_2 film; Reactive magnetron sputtering; Copper doping; Photocatalytic activity

1. Introduction

TiO_2 has been applied to a variety of environmental problems especially in water and air purification. Although TiO_2 powder has been widely used, the difficulty of recovering the powder from treated water is a major obstacle. In many studies, some research groups have immobilized TiO_2 films onto supporters to avoid further separation process [1].

Anatase TiO_2 can only absorb light below the wavelength of 387.5 nm because its band gap is 3.2 eV. In order to extend the absorption region of TiO_2 to visible light, some kinds of modification methods have been explored, such as noble metal doping [2], composite semiconductors [3], and transition metal doping [4–7]. Another purpose of surface modification of TiO_2 is to inhibit recombination of photogenerated electrons and holes by increasing the charge separation and therefore to enhance the efficiency of the photocatalytic process.

Transition metal doping has been intensively explored using the method of sol–gel, wet impregnation and co-precipitation. In most cases, the transition metals being doped in the films are in the metal oxide phases. The subsequent calcination process at high temperature results in less photocatalytic activity. Magnetron sputtering is an interesting method to prepare TiO_2 film because it is an industrial process applicable to large-area deposition, and high quality TiO_2 films can be achieved even at low substrate temperatures [8]. Therefore, it is capable to prepare transition metal doped TiO_2 films through reactive magnetron sputtering of mixed titanium and transition metal target. In our previous study, iron doped TiO_2 films were prepared through reactive magnetron sputtering of mixed titanium and iron targets [9]. In the present report, copper-doped TiO_2 films were prepared on glass substrate through Cu–Ti dc reactive magnetron sputtering. Structural and photocatalytic properties of the films were investigated.

2. Experimental

2.1. Preparation of TiO_2 film

The TiO_2 thin films were deposited on microscope glass slides (75 mm × 25 mm × 1.5 mm) by means of dc

* Corresponding author. Fax: +86 24 23893624.
E-mail address: wjzhang@imr.ac.cn (W. Zhang).

0920-5861/$ – see front matter © 2004 Elsevier B.V. All rights reserved.
doi:10.1016/j.cattod.2004.06.009

magnetron sputtering system (SBH-5115D). The dc power supplies were Advanced Energy Pinnacle 6KW and MDX Sparc-LE 20 that were set at the active arc-handling mode.

The target was titanium with purity of 99.9% and surface area of 125 mm × 378 mm. Thin copper pieces with purity of 99.9% were fixed on the titanium target. The substrates of microscope glass slides were fixed on the anode that was made of 2 mm thick steel plate. Substrate temperature was determined using a thermocouple detector on the steel plate. The distance between target and substrate was 150 mm. After the chamber was evacuated to a vacuum lower than 1.2×10^{-3} Pa, argon was introduced into the chamber and discharge began at a constant current of 2.5 A. After the discharge colour changed from pink to blue and the discharge voltage maintained at a low value, oxygen was introduced into the chamber. The argon and oxygen flow rates were 14.15 and 7.45 ml/min, respectively. All of the films were deposited for 5 h. An average film thickness of 160 nm h^{-1} could be achieved at a constant discharge current of 2.5 A.

2.2. Film characterization

The crystalline structure was measured using X-ray diffraction (XRD) with a Cu Kα source and the crystalline size was calculated using Scherrer's formula. The copper concentration was measured using electron probe microanalysis (EPMA). The surface morphology of the film was observed using scanning electron microscope (SEM). The samples for SEM imaging were coated with a thin layer of gold film to avoid charging. The titanium and copper oxidation states were determined using X-ray photoelectron spectroscopy (XPS). The optical transmission spectra of the films were measured at room temperature in air using a Shimadzu UV-265 spectrophotometer in the wavelength range from 200 to 800 nm. The thickness of the films was calculated using Swanepoel's method through UV–vis transmission spectra [10].

The photocatalytic activity of the TiO_2 films was evaluated by measuring the decomposing rate of aqueous methyl orange on the films under UV irradiation. In each experiment, a TiO_2 film of 25 mm × 25 mm was settled on the bottom of a 100 ml beaker, which contained 30 ml aqueous methyl orange. The beaker was immersed into a thermostatic bath at 30 °C. A 125 W high-pressure mercury lamp was suspended 13.5 cm above the TiO_2 films. The average intensity of UV irradiation was 4.5 mW/cm^2 by measuring with a UV irradiation meter, whose wavelength range and peak wavelength were 320–400 and 365 nm, respectively. Air was pumped into the solution at the flow rate of 100 ml/min in order to supply oxygen for the decomposition and stir the solution. Methyl orange concentration during irradiation was measured by means of Shimadzu UV-265 spectrophotometer. The initial concentration was 20 mg/l.

3. Results and discussion

3.1. Film preparation

In dc reactive sputtering, there are three oxidation modes of the target as a function of the reactive gas (O_2) flow: sputtering of metallic mode at low gas flow, compound mode at high gas flow, and transition mode in which the target changes from metallic to compound mode [11]. These different modes represent the degree of oxide coverage on the target.

While working at constant argon flow rate and discharge current, the discharge voltage increased when oxygen flow rate increased from zero up to the threshold, indicating the narrowing of the metal area being sputtered. When oxygen flow rate reached the threshold, an abrupt increase of discharge voltage occurred, due to the full coverage of oxide on the target. After that, the target voltage decreased to a stable value in the compound sputtering mode. This can be explained by an increase of the secondary electron emission yield because of the covering of the target by oxides. Only after the oxygen flow rate reached the threshold, a uniform transparent TiO_2 thin film could form on the substrate.

In order to get a series of TiO_2 samples containing different percentage of copper, pure copper pieces were fixed on the titanium target and sputtered in mixed argon and oxygen gases. After oxygen flow rate reached the threshold, the target was covered with titanium oxides and copper oxides. In order to prepare Cu-doped TiO_2 film, titanium oxides and copper oxides should be sputtered out to the substrate simultaneously during magnetron sputtering process.

Table 1 shows the copper concentration in the deposited TiO_2 films. The colour of these films changed from slight white to slight yellowish, and then to dark yellowish in the sequence from pure TiO_2 to sample B and all of the films were transparent. It can be obviously seen that, titanium oxides and copper oxides had different sputtering rates. Compared with the 125 mm × 378 mm surface area of titanium target, the fixed copper piece areas were very small, but copper concentrations were high. Therefore, it can be concluded

Table 1
Copper concentration in the Cu-doped TiO_2 films

	Sample									
	B	C	D	E	F	G	H	I	J	Pure TiO_2
Cu piece area (mm^2)	1500	750	375	180	138	102	60	30	20	0
Cu/(Cu + Ti) (at.%)	65.97	52.78	38.39	33.37	15.17	4.53	1.96	1.45	1.19	0

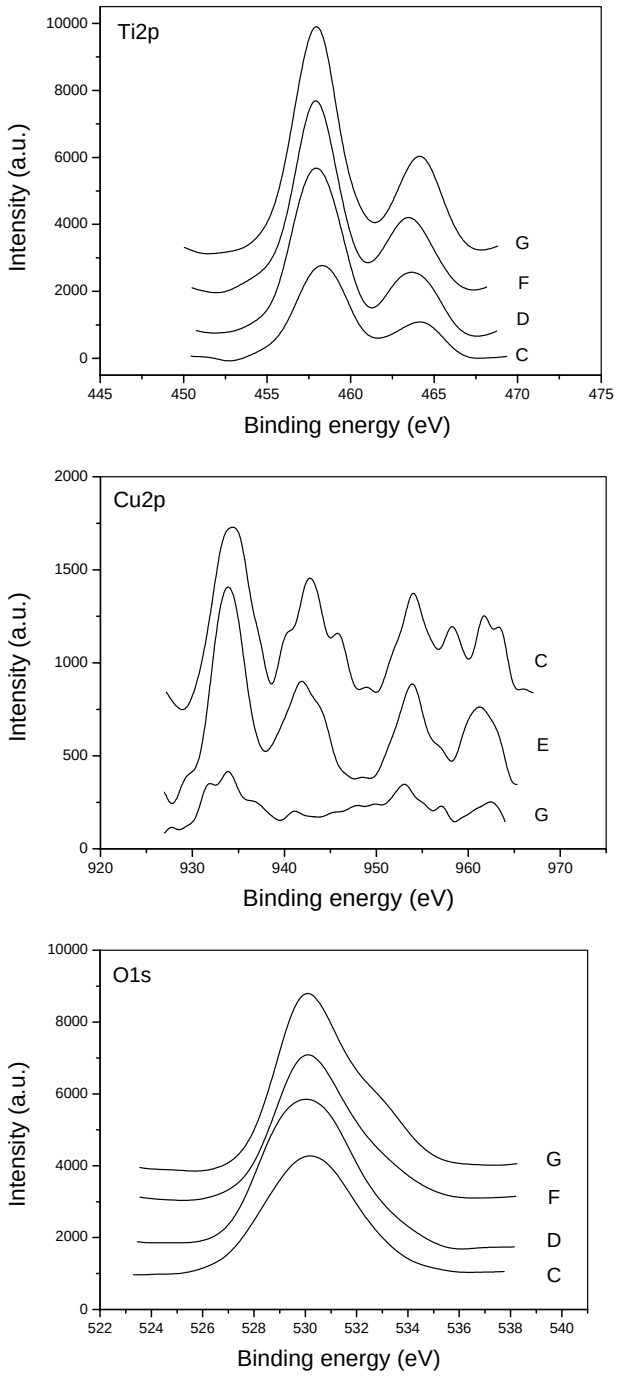

Fig. 1. XPS spectra of the Cu-doped TiO_2 film.

that copper oxides were sputtered much easier than titanium oxides.

3.2. Film characterization

Fig. 1 shows the XPS spectra of Ti 2p, Cu 2p and O 1s regions of the deposited TiO_2 film. In our experiment, only Ti^{4+} was found in the pure TiO_2 film deposited in the compound mode after oxygen flow rate surpassed the threshold. A main doublet composed of two symmetric peaks situated at Eb (Ti $2p_{3/2}$) = 458.3 eV and Eb (Ti $2p_{1/2}$) = 464.0 eV was assigned to Ti^{4+} [12]. The binding energies of Ti 2p region for the Cu-doped samples were almost as same as that for pure TiO_2 film, except that the XPS peaks were slightly broadened in highly doped films containing more than 38 at.% copper oxide. Titanium was also in the Ti^{4+} oxidation state in all the Cu-doped TiO_2 films.

The CuO was characterized by high-intensity shake-up satellites at the binding energy about 9 eV higher than the main Cu $2p_{3/2}$ and Cu $2p_{1/2}$ peaks [13]. In samples C and E with high copper concentration, the Cu 2p peaks and their satellites had high intensity, indicating the existence of fully oxidized copper oxide CuO in the films. Although the intensity of Cu 2p peaks were low in sample G because of the small amount of copper, the shake-up satellite peaks with comparably high intensity could clearly be seen in the spectra.

Oxygen of the films was in the form of O^{2-} in TiO_2 and CuO. The broadened O 1s peak to higher binding energy, which was associated with the surface hydroxide, could be seen in sample F and G with small amount of copper. The hydroxide might play an important role in the degradation process. The redox potential for photogenerated holes is +2.53 V versus the standard hydrogen electrode (SHE) [1]. After reaction with the hydroxide, these holes can produce hydroxyl radicals ($^{\bullet}OH$), whose redox potential is only slightly decreased.

Deposition temperature is a key factor of crystalline growth. The energy of the nucleation sites is a function of deposition temperature [14,15]. Although the deposition began at room temperature in our experiment, the substrate temperature could reach 110 °C after deposited for one hour and the final substrate temperature after deposited for 5 h was below 130 °C. This deposition temperature range was suitable to form quantum-sized TiO_2 film.

The XRD patterns of the pure and copper-doped TiO_2 films are shown in Fig. 2. The pure TiO_2 was in the anatase phase with the preferred orientation of (2 2 0) plane. When

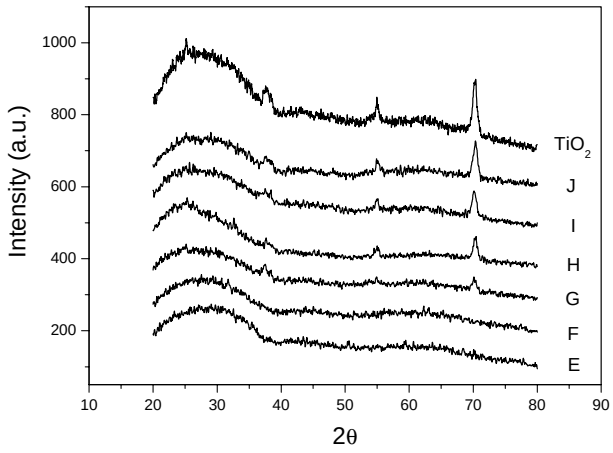

Fig. 2. XRD patterns of the pure and Cu-doped TiO_2 films.

the copper concentration was not high in samples J to G, the TiO_2 films all had the same anatase phase, although the intensity was lower than that of the pure TiO_2. The crystalline sizes in these films were below 13 nm calculated on the (2 2 0) peak of XRD patterns using Scherrer's formula. Neither oxide phase nor the preferred orientation changed in these films. The low XRD intensity of copper-doped titanium oxide film meant that the doped copper inhibited the crystal growth in the TiO_2 films. Crystalline titanium oxide could not grow in the highly copper-doped films. With copper concentration ranging from 0 up to 65.97 at.%, there was no peak of copper oxide appearing in the XRD patterns. Copper oxide was in the amorphous state in all the films even if copper concentration was higher than that of titanium.

SEM images for the surface of the Cu-doped TiO_2 films are shown in Fig. 3. In highly copper-doped sample D, the surface morphology was flat with very low roughness. As indicated in the XRD patterns, excessive doping of copper in the titanium oxide film led to amorphous mixed oxides. In sample F, which contained 15.17 at.% copper, small particles appeared on the surface of the film. When the amount of doped copper was low, the surface morphology was as similar as that of pure TiO_2 film. As shown in sample H, the film was composed of nano-crystalline TiO_2 with nano-sized pores, which could provide more surface area for photocatalytic process than flat film or films composed of large crystals.

Absorption edge of nano-sized semiconductor always shifts to lower wavelength, which is known as quantum size effects [16]. The pure and lowly copper-doped TiO_2 films perform quantum size effects due to their nano-sized crystalline structure, as shown in Fig. 4. The absorption edges of the Cu-doped samples shifted to longer wavelength region and the optical transmittances of these films decreased abruptly with increasing copper concentration. This was caused by two factors. One reason is that copper oxide can absorb light with longer wavelength because its band gap is around 2.0 eV. The doped copper oxide expanded the absorption range within light spectrum, so that more of light irradiation could be used in photocatalytic process.

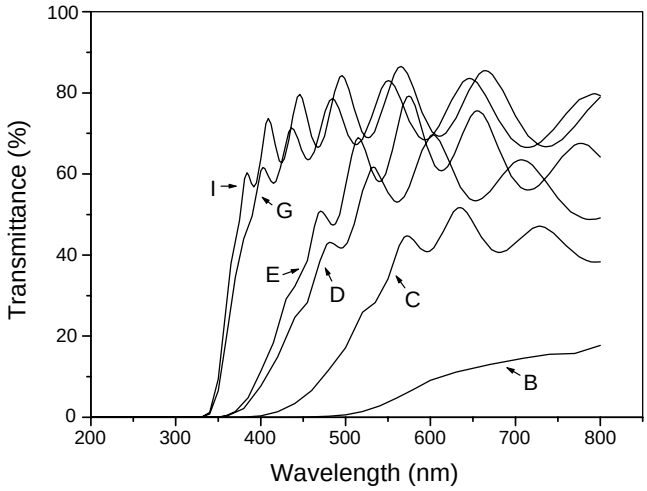

Fig. 4. UV–vis spectra of the Cu-doped TiO_2 films.

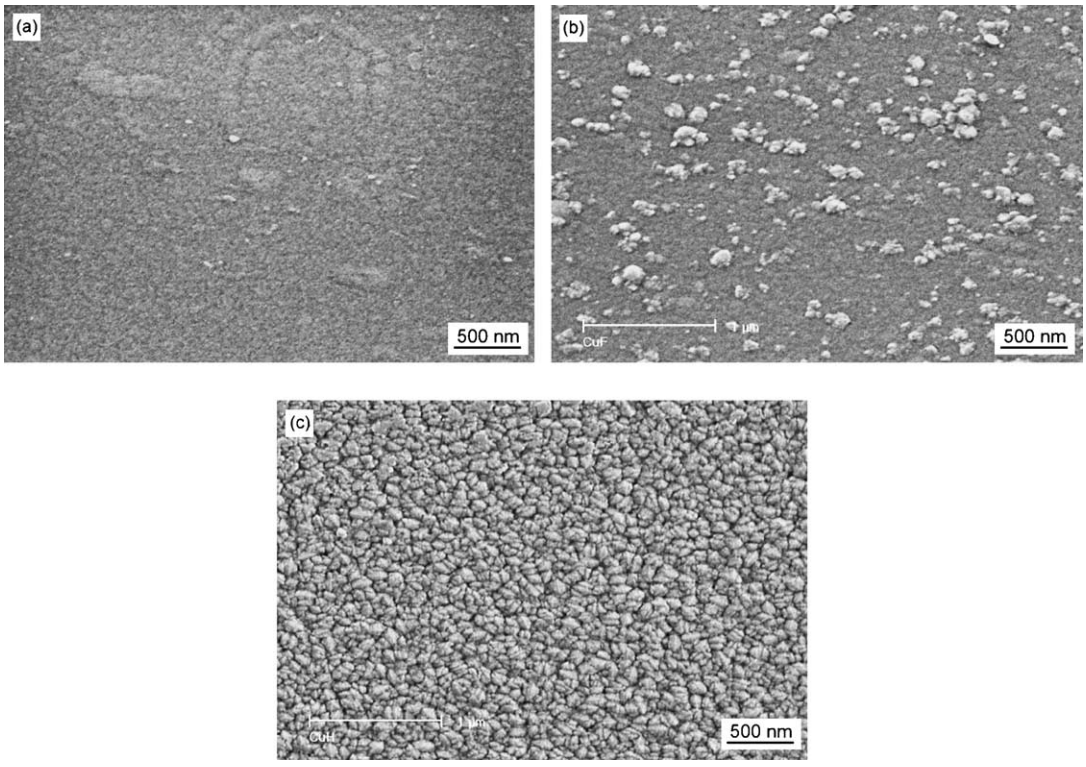

Fig. 3. SEM images of the Cu-doped TiO_2 films: (a) D, (b) F, and (c) H.

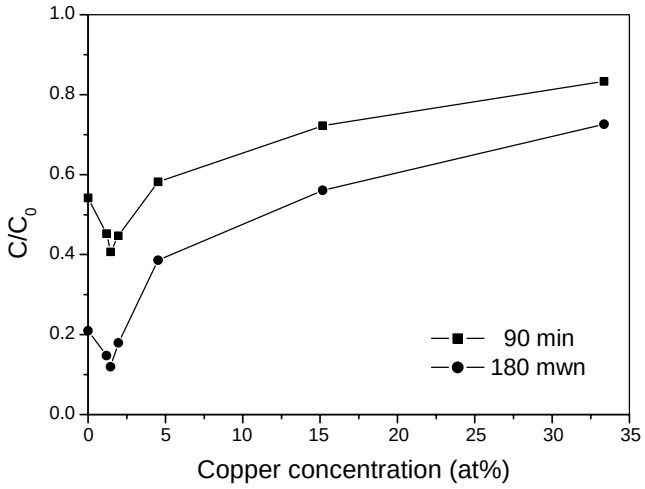

Fig. 5. Photocatalytic degradation of methyl orange on the Cu-doped TiO_2 films (C_0 is the initial aqueous methyl orange concentration of 20 mg/l and C is the aqueous methyl orange concentration after 90 or 180 min irradiation).

Another reason is that, within the semiconductor, the extinction of light follows the exponential law: $I = I_0 \exp(-al)$. Where l is the penetration distance of the light and a is the reciprocal absorption length [17]. The films have different a at same wavelength, which results in different light extinction rate. For pure TiO_2, a has the value $2.6 \times 10^4\ cm^{-1}$ at 320 nm. The extinction rate increased with the increasing amount of doped copper in the TiO_2 films, leading to rapid transmittance decreasing for highly doped films.

3.3. Photocatalytic activity

In this report, aqueous methyl orange degradation is used to determine the photocatalytic activity of the copper-doped TiO_2 photocatalysts. The photocatalytic decomposition follows first-order kinetics in the adsorbed concentration of methyl orange on the surface of titanium oxide films.

After light absorption with energy equal to or greater than the band gap of the semiconductor, electrons and holes are generated. In competition with charge transfer to adsorbed species is electron and hole recombination. The doped copper can provide a shallow trap for photo-generated electron and hole so as to inhibit the recombination and extend the lifetime of charge carrier. Therefore, the photodegradation rate could be enhanced consequently because more charge carriers are available.

Fig. 5 shows the methyl orange degradation rates during 180 min irradiation on the Cu-doped TiO_2 films compared with the pure TiO_2 film. The Cu-doped TiO_2 films had different photocatalytic behavior in accordance with the amount of doped copper. The optimum copper doping concentration was 1.45 at.% in sample I, which showed the most effective photocatalytic activity. When the copper concentration surpassed the optimum value, the photocatalytic activity decreased sharply, which was even lower than that of the pure TiO_2 film. This optimum concentration can be explained by the balance of an increase in trapping sites leading to efficient trapping and fewer trapped carriers leading to longer lifetimes for interfacial charge transfer [18]. At lower concentration below the optimal value, photocatalytic activity increased with an increasing copper concentration because there were fewer trapping sites available.

4. Conclusions

Copper-doped titanium oxide films were prepared by dc magnetron sputtering method using Ti and Cu mixed target. The XPS spectra of Ti 2p region showed that titanium was in the Ti^{4+} oxidation state in all the Cu-doped TiO_2 films. Apparent high-intensity shake-up satellites at higher binding energy than the main Cu 2p peaks indicated the existence of fully oxidized CuO in the films. Oxygen of the film was in the form of O^{2-} in TiO_2 and CuO.

When the copper concentration was low, the Cu-doped TiO_2 films had the similar anatase phase as the pure TiO_2. The samples became amorphous when copper concentration was more than 15.17 at.%. Copper oxides were in the amorphous state in all the films, with copper concentration ranging from 0 up to 65.97 at.%. The surfaces of the Cu-doped TiO_2 films represented different morphologies, from flat to nano-crystalline with nano-sized pores, in the sequence of decreasing copper concentration.

The absorption edges of the Cu-doped samples shifted to longer wavelength region and the optical transmittance decreased abruptly with increasing copper concentration. The Cu-doped TiO_2 films had different photocatalytic behavior in accordance with the amount of doped copper. The optimum copper doping concentration was 1.45 at.% in sample I, which showed the most effective photocatalytic activity.

Acknowledgements

This work was supported by the National Natural Science Foundation of China (No. 50001013), Hundred-talent Project of CAS and the NSFC for Outstanding Young Scientists (No. 59625103).

References

[1] A. Fujishima, T.N. Rao, D.A. Tryk, J. Photochem. Photobiol. C1 (2000) 1.
[2] T. Sasaki, N. Koshizaki, S. Terauchi, H. Umehara, Y. Matsumoto, M. Koinuma, Nanostruct. Mater. 8 (1997) 1077.
[3] C. Hu, Y.Z. Wang, H.X. Tang, Appl. Catal. B 30 (2001) 277.
[4] K. Chiang, R. Amal, T. Tran, Adv. Environ. Res. 6 (2002) 471.
[5] Z.H. Yuan, J.H. Jia, L.D. Zhang, Mater. Chem. Phys. 73 (2002) 323.
[6] M.I. Litter, Appl. Catal. B 23 (1999) 89.

[7] A.D. Paola, E. García-López, S. Ikeda, G. Marcì, B. Ohtani, L. Palmisano, Catal. Today 75 (2002) 87.
[8] W.J. Zhang, Y. Li, F.H. Wang, J. Mater. Sci. Technol. 18 (2002) 101.
[9] W.J. Zhang, Y. Li, S.L. Zhu, F.H. Wang, Chem. Phys. Lett. 373 (2003) 337.
[10] R. Swanepoel, J. Phys. E 16 (1983) 1214.
[11] R. Gouttebaron, D. Cornelissen, R. Snyders, J.P. Dauchot, M. Wautelet, M. Hecq, Surf. Interf. Anal. 30 (2000) 527.
[12] J. Pouilleau, D. Devilliers, H. Groul, J. Mater. Sci. 32 (1997) 5645.
[13] S. Poulston, P.M. Parlett, P. Stone, M. Bowker, Surf. Interf. Anal. 24 (1996) 811.
[14] Y.Z. Cheng, Y.M. Zhang, Y. Tang, Chin. J. Catal. 22 (2001) 203.
[15] X.Y. Yu, J.J. Cheng, J. Inorg. Mater. 16 (2001) 742.
[16] A.L. Linsebigler, G.Q. Lu, J.T. Yates, Chem. Rev. 95 (1995) 735.
[17] A. Hagfeldt, M. Gratzel, Chem. Rev. 95 (1995) 49.
[18] W. Choi, A. Termin, M.R. Hoffmann, J. Phys. Chem. 98 (1994) 13669.